

Evaluation of BCECF fluorescence ratio imaging to properly measure gastric intramucosal pH variations *in vivo*

Philippe Rochon

Lille University Hospital
Pavillon Vancostenobel
59037 Lille Cedex, France

Mercé Jourdain

Jacques Mangalaboyi

François Fourrier

Lille University Hospital
"Service de Réanimation Polyvalente"

Sylvie Soulié-Bégu

UMR CNRS/ENSCM/UM1 5618
Montpellier, France

Bruno Buys

Guy Dehlin

Jean Claude Lesage

Marie Christine Chambrin

Serge Mordon

Lille University Hospital
INSERM (French National Institute of Health
and Medical Research)
Lille, France

Abstract. Our purpose is to evaluate intramucosal gastric pH video imaging by 2',7'-bis(carboxyethyl)-5,6-carboxyfluorescein (BCECF) fluorescence ratio techniques. We use a video endoscopic imaging system and BCECF as the pH fluorescent probe. Systemic *in vivo* pH variations are studied in 10 pigs: five in the control group and five with respiratory acidosis induced through rebreathing. The intramucosal pH of the gastric wall is measured every 5 s and the results demonstrate a good correlation (pearson correlation=0.832) between blood gases pH measurements and pH measured with the video endoscopic imaging system. Our results confirm the feasibility of using BCECF fluorescence pH imaging to measure intramucosal pH *in vivo*. © 2007 Society of Photo-Optical Instrumentation Engineers. [DOI: 10.1117/1.2821698]

Keywords: medical imaging; fluorescence; endoscopy; image processing.

Paper 07173R received Jun. 8, 2007; revised manuscript received Jul. 30, 2007; accepted for publication Aug. 18, 2007; published online Dec. 14, 2007.

1 Introduction

The measurement of gastric intramucosal pH (pH_{im}) provides a measure of tissue acid balance in a region of the body that is among the first to develop dysoxia during shock states. The degree and duration of these episodes of gastric intramucosal acidosis are highly sensitive measures of the risk of developing injured and "leaky" gut and its putative consequences, namely translocation, cytokine release, organ dysfunction and failure, sepsis, and death from organ failure.¹ Gastric mucosal ischemia due to diversion of blood flow to vital organs has been shown to develop in critically ill patients in a number of clinical settings and can be detected by measurement of gastric pH_{im}. Previous studies have shown that a decrease in pH_{im} predicts the occurrence of gastrointestinal bleeding, postoperative complications, sepsis, failure to wean from mechanical ventilation, and increased mortality.^{2,3} It has been shown that the existence of abnormal pH_{im} in sepsis patients transferred to intensive care unit (ICU) was associated to 87% mortality. An accurate measurement of gastric pH_{im} could provide advanced warning of the putative consequences of dysoxia and enable early preventive intervention.^{4,5}

While blood pH measurement methods have existed for over 40 yr, little progress has been achieved in measuring the pH_{im} in a noninvasive and continuous way. Measurements of gastric pH_{im} remain an issue in ICU. The development of indirect pH_{im} measurements such as the tonometric method, where the pH_{im} is obtained by measuring both PCO₂ in the lumen of the gut with a silicone balloon as well as bicarbonate concentration in arterial blood and substituting these two values in the Henderson-Hasselbach equation, has failed to provide the ICU departments a reliable and fast pH_{im} measurement method.

A major advance in accurate *in vivo* pH measurement was the development of the ratiometric fluorescent probe, 2',7'-bis(carboxyethyl)-5,6-carboxyfluorescein (BCECF) (BCECF mixed isomers B-1151 Molecular Probes). BCECF excitation spectra is pH dependant in the range 5 to 8 (Fig. 1), which is particularly adapted to study^{6,7} physiological pH. Since its introduction by Tsien,⁸ BCECF has become one of the most used fluorophore for pH determination. With a fluorescence efficiency of 92%, BCECF presents excellent properties of fluorescence. The use of BCECF for the determination of the pH *in vivo* was validated in a number of studies.^{9,10} The pH-dependent spectral shifts exhibited by BCECF enable calibration of responses in terms of ratio of fluorescence in-

Address all correspondence to Serge Mordon, PhD, INSERM & Lille University Hospital, Pavillon Vancostenobel, 59037 Lille cedex, France; Tel: +33 320 446 708; Fax: +33 320 446 708; E-mail: mordon@lille.inserm.fr

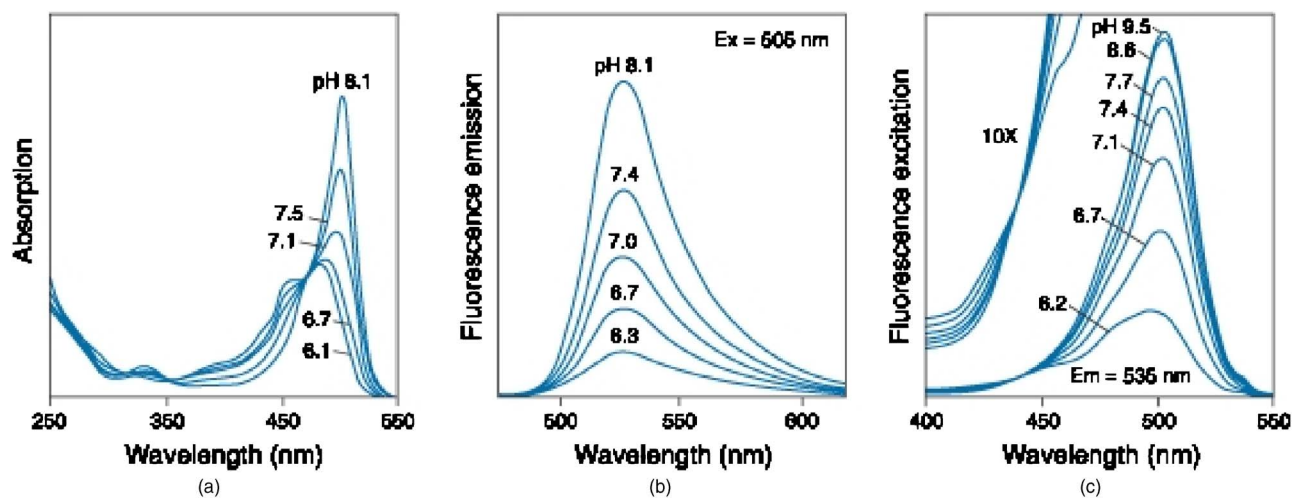


Fig. 1 BCECF (A) absorption, (B) emission, and (C) excitation spectra.

tensity measured at two different excitation wavelengths. This ratio of fluorescence eliminates measurements artifacts including photobleaching, leakage, nonuniform loading of the indicator, and instrument stability.^{11,12} The fluorescence ratio imaging technique has long been well understood.^{6,13,14} This technique enables quantification and immediate functional imaging of physiological parameters.

Since 1995, our laboratory has been developing a pHim imaging technique based on the specific fluorescent properties of BCECF. Preliminary studies were carried out in our laboratory to study the *in vitro* BCECF calibration curve, the *in vivo* pharmacokinetics of BCECF, the variation of the fluorescence level according to the probe concentration, the variation of the fluorescence level according to the intensity of the excited light, and the *in vivo* variations of the ratio of fluorescence according to the rate of hematocrit or of protein concentrations.^{6,15,16} These studies made it possible to determine the range of linearity of the BCECF fluorescence emission required to perform ratio imaging. They also demonstrated that the acid form of BCECF remains largely in the extracellular space owing to its relatively low membrane permeability, and its excretion is consistent with an extracellular localization.

This experimental study aims to evaluate the accuracy of the BCECF fluorescence ratio imaging to measure sequential pHim variations *in vivo*. Respiratory acidosis induced by re-breathing is used to induce systemic pH variation.

2 Materials and Methods

2.1 Animals

Pigs used in this study were female “large white” pigs, weighting 20 to 25 kg, obtained from a breeding farm. This study was approved by the Institutional Review Board of animal research. Care and handling of the animals were in accordance with National Institutes of Health guidelines. All pigs had no access to food the night before the day of experiment, but they had free access to water.

2.2 Anesthesia and Surgical Preparation

The animals were premedicated with intramuscular injection of ketamine 2.5 mg/kg body weight (Ketalar®, Parke-Davis, Courbevoie, France) and 0.25 mg/kg body weight midazolam (Hypnovel®, Produits Roche, Neuilly/Seine, France) enabling insertion of an earlobe marginal venous catheter. Anesthesia and curarization were induced by 10 mg/kg body weight pentobarbital sodium injection (Nesdonal®) and pancuronium (Pavulon, 0.2 mg/kg). After anesthesia, the animals were placed in supine position and each trachea was intubated with a cuffed tube (Portex, 7.5 mm diameter) and connected to a pressure-controlled ventilation unit (Evita 1, Dräger Medical, Lübeck, Allemagne). During the experiment, animals were anesthetized with a continuous infusion of 0.5 $\mu\text{g}/\text{kg min}^{-1}$ of midazolam. Muscle relaxation was obtained by a continuous infusion of 0.5 $\mu\text{g}/\text{kg min}^{-1}$ pancuronium bromide (Pavulon®, Organon Teknika, Fresnes, France). After the dissection of neck vessels, a Swan Ganz oxymetric catheter (Baxter 130 H 7.5F 777F8 Baxter Edwards Critical Care, Irvine, California) was positioned in the pulmonary artery via the right external jugular vein, its position being determined by the typical pressure tracing on the monitor. Another catheter (Arrow 8 Fr, PA, USA) was introduced in the left carotid artery for continuous blood pressure monitoring and blood sampling. The endoscope (GIF XQ40, Olympus, Rungis, France) was introduced into the stomach at the end of the surgical procedure. Heat lamps suspended above the operating table were used to ensure a central venous blood temperature of $37.5 \pm 0.8^\circ\text{C}$.

2.3 Hemodynamics and Oxygen Transport

For all animals, hemodynamics [heart rate (HR), arterial pressure (AP), peak airway pressure (PaP), and cardiac output (CO)], oxygenation [venous oxygen saturation (SvO_2) and end-tidal carbon dioxide (ETCO_2)], and ventilation parameters [tidal volume, minute ventilation, fractional concentration of oxygen in inspired gas (FiO_2)] were recorded continuously. Standard cardiometer (PC Express TM 90308,

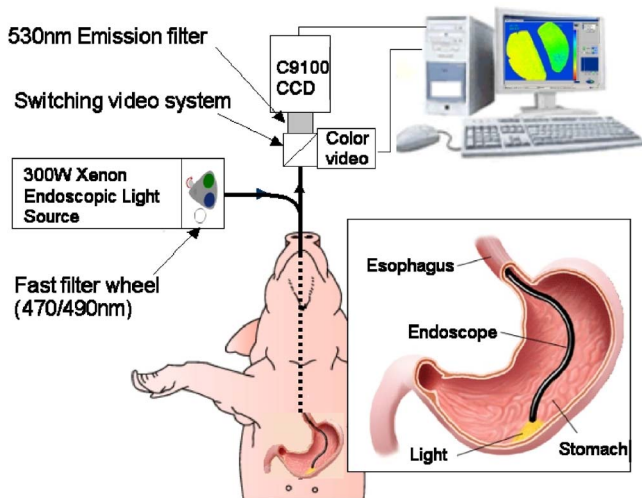


Fig. 2 Fluorescence imaging system.

Spacelabs Medical Inc., Redmond, Washington), Swan Ganz (Baxter 130 H 7.5F 777F8 Baxter Edwards Critical Care, Irvine, California), and Cosmo (Novamatrix, Wallingford, Connecticut) were used. Arterial and venous blood samplings were drawn simultaneously from carotid and pulmonary arteries for blood gas (BG) analysis. Arterial and venous BGs were measured in an acid-base analyzer (ABL-520, Radiometer, Copenhagen, Denmark) at 37°C. Arterial and venous lactate concentrations were measured in a lactate analyzer (Hitachi Analyzer 717, BioMérieux kit; Lyon, France).

2.4 pHim Measurement

The fluorescence imaging system is shown on Fig. 2. Measurements were realized on the fundus gastric mucosa. In the pig, this mucosa covers the great curve and the body of the stomach. The field of view was around 20 cm² and the endoscope remained in the same position. After

BCECF intravenous injection (2',7'-bis(2-carboxyethyl)-5(6)-carboxyfluorescéine, Laboratoires Synth-Innov, Paris, France), the fluorescent probe was successively excited at two different wavelengths (470 to 490 nm) using a fiber optical endoscope (GIF XQ40, Olympus, Rungis, France) and a customized 300-W xenon endoscopic light source (EXERA CLV-160, Olympus, Rungis, France). It was modified and equipped with a fast filter-switching system (switching times less than 20 ms).

The resulting fluorescence images were collected using an EMCCD camera (C9100-12 EMCCD, Hamamatsu Photonics, Massy, France). Exposure times were 100 ms/image to achieve good superposition of the two successive images used to compute the ratio image. Each acquisition sequence was triggered with the ventilator unit signal and was obtained at the end of the exhalation cycle, as described in Fig. 3.

Before each new experiment, the ratio of excitation intensity $R_{cal} = I_{490}/I_{470}$ was measured. The CCD camera dark signal (CCDDS) was also measured. The fluorescence ratio image was computed, pixel by pixel, using the following formula:

$$ratio(x,y) = \frac{I_{490}(x,y) - CCD_{DS}}{I_{470}(x,y) - CCD_{DS}} \cdot \frac{1}{R_{cal}}$$

The following *in vitro* calibration curve (see Fig. 4) was used to convert ratio (x,y) values to pH(x,y) values¹⁵:

$$pH(x,y) = pK_a + \log \left[\frac{ratio(x,y) - R_{min}}{R_{max} - ratio(x,y)} \right],$$

with $pK_a = 6.97$, $R_{min} = 1.02$, and $R_{max} = 2.18$.

For each resulting image, the pHim was automatically measured on a centered circular region of interest (around 1 cm² of mucosa). A single pH value was obtained by averaging all pH(x,y) values included in the region of interest. An

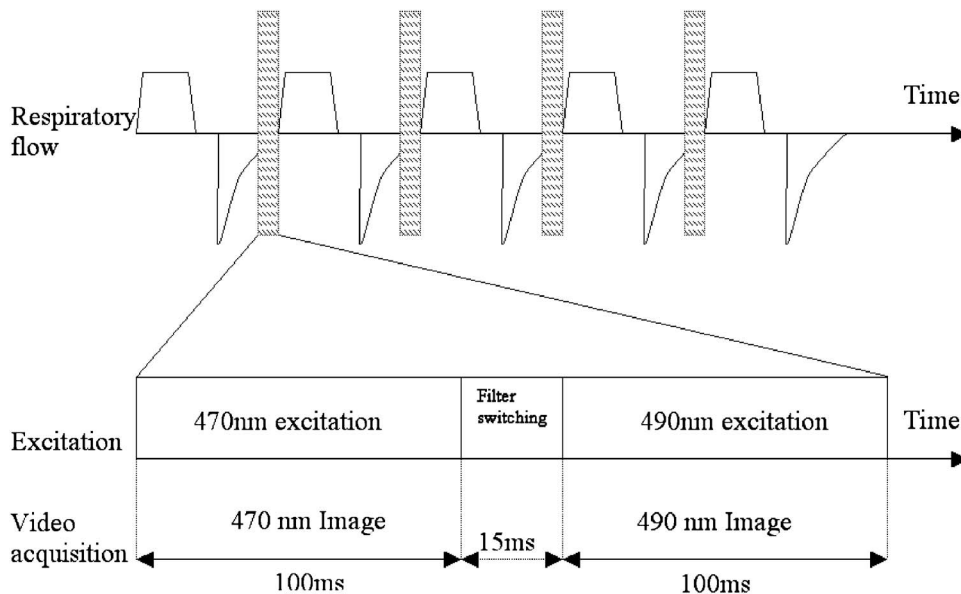


Fig. 3 Timing of the image acquisition sequences.

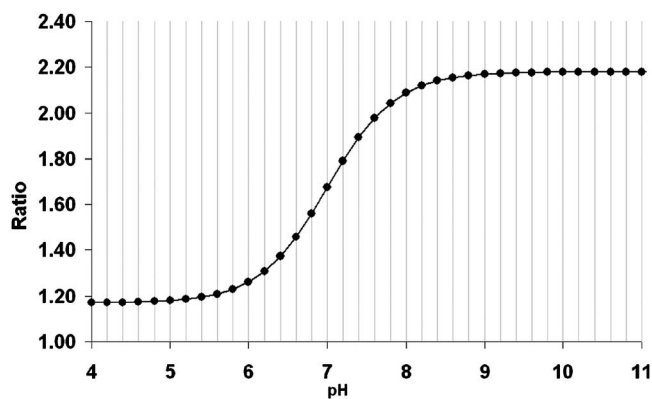


Fig. 4 *In vitro* BCECF calibration curve of the ratio of fluorescence emitted at 532 nm resulting from a 490- and 470-nm excitation.

example of classic color video image and pH images with region of interest are shown on Fig. 5.

2.5 Experimental Protocol

BCECF at 4 mg/kg of body weight was diluted in 20 ml HCO_3^- , 8.4% solution. After a 1-h period of stabilization following animal surgical preparation, BCECF was injected intravenously from $T=0$ to $T=1$ min. Between $T=1$ and $T=60$ min a new stabilization period was observed, enabling us to compare the baseline value of each group. Between $T=60$ to $T=240$ min, studies were performed in two groups of five pigs. The control group received only BCECF. In the respiratory acidosis group, the animals underwent two hypercapnia episodes of 20 min at $T=60$ min and $T=140$ min. Hypercapnia and respiratory acidosis were induced by the addition in the respiratory circuit of a 300-mL dead space while FiO_2 was set to 100% to avoid hypoxemia. The animals were constantly ventilated without changing ventilation parameters. In each group, pHim, hemodynamics, oxygenation, and ventilation parameters were continuously recorded between $T=0$ and 240 min.

2.6 Statistical Methods

Statistical results were given as mean \pm standard deviation (St Dev). Because of limited number of samples, nonparametric tests were used to analyze the data. A Wilcoxon matched-pairs signed-rank test (W) was used to analyze significant variation in groups. The Pearson correlation coefficient was used to determine correlation coefficient moment for pairs of variables and the Kruskal-Wallis (KW) test was used to study intergroup variation at $T=60$ min.

3 Results

No side effects were observed after BCECF injection in our animals. Clinical tolerance was excellent. We could not observe any hemodynamic changes during intravenous BCECF administration. Only a rapid and transient increase of ETCO_2 due to the dilution of the molecule in HCO_3^- -buffer was recorded. Fluorescence reached its maximum a few seconds after injection (10 to 20 s) and decreased as a function of time. Diffusion in the gastric tissue was instantaneous and was confirmed by fluorescence detection through endoscopic imaging. Conversely, no fluorescence was detected in the gastric lumen. A 4-h observation period was carried out for each group. Approximately 2500 successive pHim measurements were performed for each pig. To better read the figures and compare with blood sample pH measurement, only data obtained at key times regarding each group protocol were plotted— $T=5, 15, 30, 60, 120, 180,$ and 240 min for control group [Fig. 6(a)], and $T=5, 15, 30, 60, 80, 140, 160,$ and 220 min for the respiratory acidosis group [Fig. 6(b)].

During the 1-h period of stabilization after BCECF injection, no significant intergroup difference was observed (KW at $T=60$ min pHim: $p=0.076$, ApH: $p=0.282$, and VpH: $p=0.203$). Results, as discussed next, are summarized in Table 1.

3.1 Control Group

The monitoring parameters were stable during 4 h. No significant clinical variations were observed. The pHim values are plotted in Fig. 6(a). Two phases were observed: a rising phase from $t=0$ to 30 min, and a plateau phase from $t=30$ to

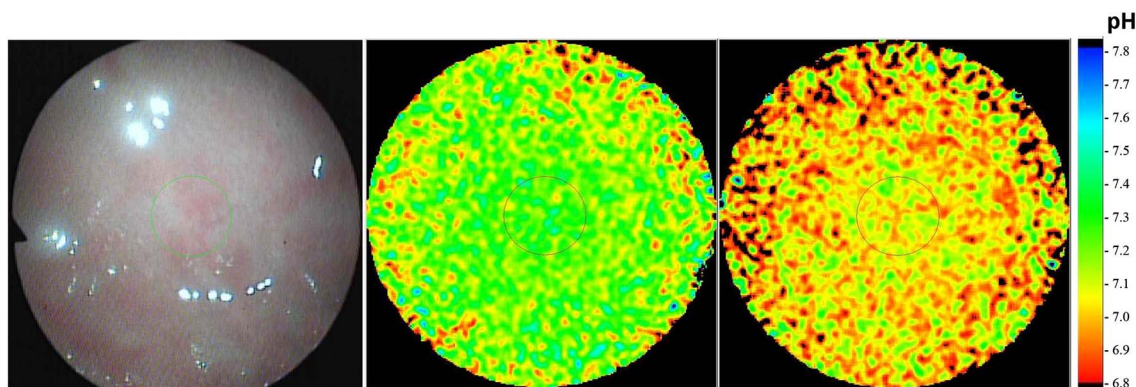


Fig. 5 Example of images obtained on a pig of hypercapnia group. From left to right: classic color video image of mucosa at $T=60$ min, pH image of mucosa at $T=60$ min during hypercapnia event, and pH image of mucosa at $T=160$ min during hypercapnia. The circle represent the region of interest.

Table 1 Averaged pHim, arterial and venous pH BGs, and arterial and venous lactate for the control and hypercapnia groups.

Control Group (min)	5	15	30	60	90	120	150	180	210	240
pHim	7.13	7.23	7.27	7.28	7.28	7.29	7.28	7.29	7.27	7.27
ABG pH	7.44			7.43		7.43		7.46		7.45
VBG pH	7.41			7.40		7.41		7.42		7.42
PaCO ₂	41			45		50		45		47
PvCO ₂	47			51		49		48		47
Hypercapnia Group (min)	5	15	30	60	80	110	140	160	190	220
pHim	7.18	7.29	7.32	7.31	7.17	7.27	7.27	7.05	7.15	7.21
ABG pH	7.43			7.43	7.04		7.40	7.04		7.38
VBG pH	7.38			7.39	7.07		7.35	7.04		7.34
PaCO ₂	47			49	126		51	133		58
PvCO ₂	53			52	118		59	127		64

240 min (pHim=7.36±0.05 for 30 min to 4 h after injection). In the same figure, arterial pH (ABGpH) and venous pH (VBGpH) values are shown. Mean arterial pH was 7.44±0.01 and mean venous pH was 7.41±0.02. BG pH standard deviations were very small (<0.02 data not shown). Lactate levels were in the range 1 to 2 mmol/L. Bicarbonate levels were stable (arterial: 29 mmHg±2 mmHg; venous: 30 mmHg±2 mmHg).

3.2 Hypercapnia Group

Each hypercapnic event produced a decrease in pHim, from 7.36±0.10 to 7.17±0.11 during the first episode, and from 7.27±0.08 to 7.05±0.04 for the second episode, respectively [Fig. 6(b)]. In both cases, the pHim decrease was significant with regards to the Wilcoxon signed rank test ($W=15$). ApH and VpH values decreased, respectively, from 7.41±0.05 to 7.03±0.04 and 7.38±0.05 to 7.02±0.05 during the first hypercapnia event and from 7.37±0.05 to 7.05±0.05 and 7.32±0.08 to 7.04±0.03 during the second event. Figure 6 presents classic color video images, and pH images obtained at $T=60$ min and $T=160$ min. During the 1-h recovery time, both BGpH and pHim did not fall back to their initial baseline, but variations compared to the $T=60$ min reference baseline were not significant for both pHim and BGpH measurements. Between $T=60$ min and $T=220$ min, the Pearson correlation coefficient of pHim and arterial BGpH samples was 0.832, and that of the pHim and venous BGpH samples was 0.795. During hypercapnia, EtCO₂ reached a maximum: 134±21 mmHg at the end of the first hypercapnic period and 142 mmHg±23 mmHg during the second (data not shown). Lactate levels were stable in the range 1 to 2 mmol/L. Bicarbonate levels tended to increase slightly (data not shown) during hypercapnia event, but variations were not significant.

4 Discussion

The gut is the organ with the highest critical oxygen delivery (DO₂) in the body. Since the gut is richly innervated by the sympathetic nerve system, the response to a decrease in global DO₂ such as during hemorrhagic aortic occlusion or hepatic vascular exclusion, intestinal vasoconstriction is greater than most vascular beds when blood is redistributed to the vital organs and may persist when systemic hemodynamic variables have been reestablished. These conditions jeopardize the integrity of gut mucosal cells, predisposing it to increases in gut permeability and translocation of bacteria and their toxins. The direct measurement of pHim provides a measure of pH in the most superficial layer of the mucosa, a region of the gut rendered relatively hypoxic by the countercurrent exchange system within the mucosal vasculature and hence especially sensitive to alterations in the adequacy of tissue oxygenation.

The technique used in this study was already evaluated by Russel et al.¹⁰ They developed a noninvasive optical fiber system for *in vivo* pH measurements after BCECF injection in conscious mice. The target tissue was excited alternately at 450 and 500 nm. The emitted fluorescence was measured by a photomultiplier tube. They measured the extracellular pH in hairless mice exposed to elevated partial pressure of CO₂. They demonstrated changes in the fluorescence signal indicative of a dramatic decrease in extracellular pH. With brief exposure, the pH recovered within 20 min. Similarly, Marechal et al.⁶ validated a similar fluorescence imaging technique to measure *in vivo* pHim of rat exteriorized intestine, with an accuracy of 0.07 pH unit.

To test our video imaging system, we chose a protocol of systemic pH variation. The objective of such protocol was to induce rapid and uniform acidosis in the tissue compartment to test the pHim imaging system sensitivity and response time.^{17,18} Our results show that a rising time about 15 to

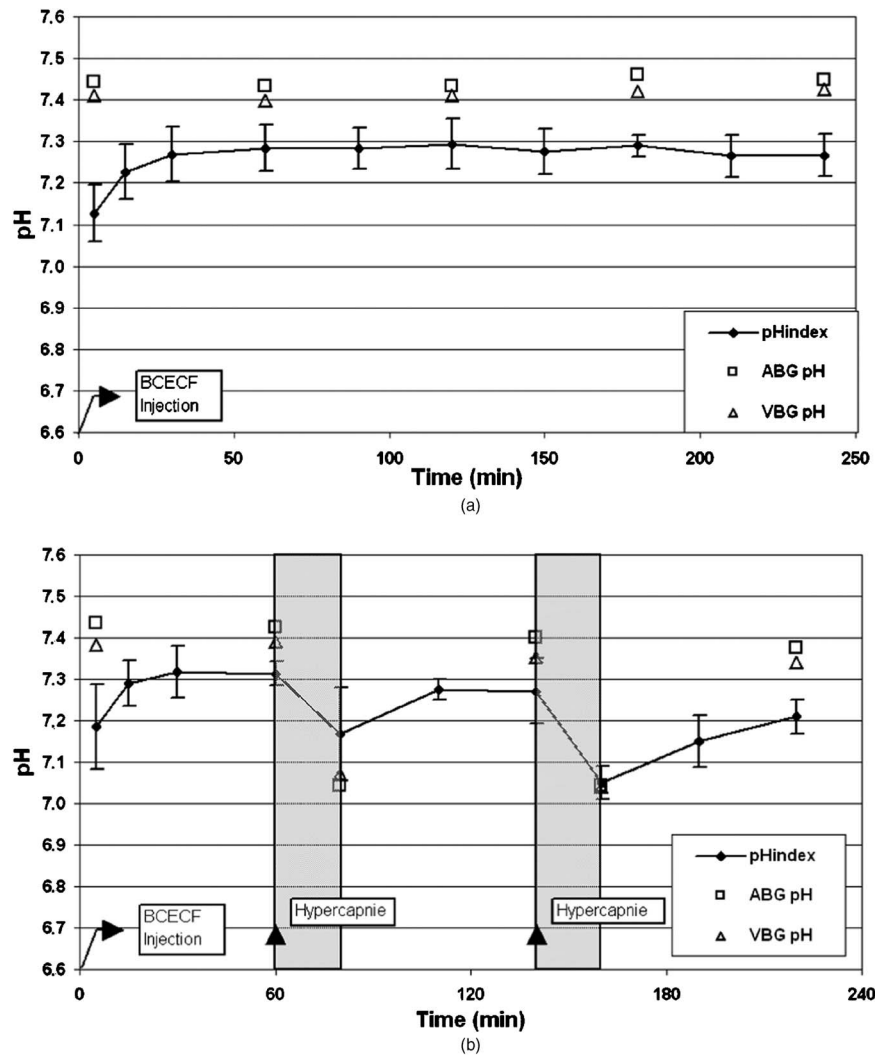


Fig. 6 Averaged pHim and ABGpH/VBGpH for (a) the control group ($n=5$) and (b) the hypercapnia group ($n=5$) (Rq: BG standard deviation are not represented for readability; standard deviations were less than 0.02 for the control group and 0.05 for the hypercapnia group). For better readability of figures and comparison with pH blood sample measurement, only the data obtained at key times regarding each group protocol are plotted [$T=5, 15, 30, 60, 120, 180,$ and 240 min for the control group (a), and $T=5, 15, 30, 60, 80, 140, 160,$ and 220 min for the respiratory acidoses group (b)].

30 min after BCECF injection is necessary in order to be able to use pHim results. It does not appear that this rising time is related to a characteristic of diffusion of the BCECF in tissue, since fluorescence is observed in the gastric tissue less than 1 min following the injection. It could be assumed that this rising time is potentially related to the strong BCECF concentration following the injection, leading to a transitory phenomenon in the quenching of fluorescence. This period of time could be probably reduced by better control of light excitation just after injection, or by infusing BCECF more slowly.

From 70+30 min to the end of experiment, the reproducibility and stability of pHim measurements were good in the control group. Variations due to tissue motion were very limited. The value of pHim remained within a normal range for the duration of the experiment. These results tend to validate the timing used to realize the image acquisition. Nevertheless, a small variation between blood sample pH and pHim was

observed. Several hypotheses can be formulated to explain this variation. On the instrumental side, a small mismatch of the calibration curve can induce an offset in the measurement. The delicate point of these experiments lies in the calibration of the pHim mapping system. To our knowledge, there is no simple and nontraumatic technique available to measure tissue pHim simultaneously with mapping pHim measurement. Antonsson and Boyle¹⁹ tried to measure pHim by means of microelectrodes inserted in the wall of gastric tissue, but the technique is fairly unreliable and challenging to use. Specific issues include difficult calibration; drift problems; tissue and protein buildup, easily clogging the reference junction; positioning issues; and more important, the modification of local pHim by tissue damage induced by the pH probe insertion.

Another issue is that pHim seems not to be within range (VBGpH to ABGpH). Several studies using tonometric measurement present a gradient of PCO_2 between intramucosal tissues PCO_2 and arterial, mixed venous or portal venous

PCO₂. For instance, Guzman and Kruse²⁰ found a baseline PiCO₂ to PaCO₂ equal to 16.9±3.3 mmHg. Using the Henderson-Hasselbach equation, such an offset would produce an offset of 0.15 pH unit. Those results are in good agreement with ours. Similarly, pH measurements realized by Puyana et al.⁵ on the dog stomach mucosa using microelectrodes (7.17) and air-equilibrated tonometer (7.26) while arterial pH was 7.475 are in keeping with our results.

During the hypercapnia challenge, blood sampling shows that arterial and venous pH blood gases decrease when PCO₂ increases. Our results show good correlation (correlation=0.832) between BGpH and pHim dynamics, enabling us to conclude that the ratio imaging system is sensitive to pHim modifications. During the first hypercapnia challenge, our results show that the pHim is less reduced (7.24) than the arterial (7.04) and venous pH (7.07). This observation was expected because of progressive CO₂ accumulation by the gut tissue. Guzman and Kruse showed that the variation of intramucosal PCO₂ are not as fast as the variations²⁰ of PaCO₂. Similarly, since additional CO₂ was not completely eliminated after the first hypercapnia challenge, pHim was not restored to its initial value before the start of the second hypercapnia challenge. At the end of the second challenge, the pHim was reduced to the values observed for the arterial and venous pH blood. Again, due to an important CO₂ retention by the tissue, the pHim was not restored to its initial value 1 h after the stop of the second hypercapnia period.

5 Conclusion

We clearly demonstrated that pHim endoscopic imaging using BCECF as a pH fluorescent indicator is feasible. The pHim is directly measured and not calculated, as is the case with tonometry. Measurement is not averaged from the entire stomach wall, but local pHim variations can be detected, depending only on the optical resolution of the endoscope. Measurements are not obtained every 30 min, but every 5 s.

Besides its obvious potential in an ICU to detect the circulatory status of critically ill patients through its reliable evaluation of splanchnic and peripheral perfusion,²¹ this technique could be very useful in determining the adequacy of splanchnic perfusion and as endpoints to guide therapeutic intervention. For example, Masai et al. showed that intraoperative monitoring of pHim is useful for the evaluation of visceral organ ischemia during surgery.²²

Further experiments will evaluate this new imaging technique to quantify pHim during endotoxemic shock, severe hypoxia, or hemorrhagic shock and possibly in more specific applications into surgery.

Acknowledgments

The assistance of Synth InnoVe (F. Scherninski) is gratefully acknowledged. Grants were awarded by the OSEO-ANVAR (No. A0304067), ANR (No. 06 EMPB-024-01) by the Institut National de la Santé et de la Recherche Médicale (Inserm), and by the University Hospital of Lille. The authors wish to thank Pascal Servell for careful reading of the manuscript.

References

1. R. G. Fiddian-Green, "Gastric intramucosal pH, tissue oxygenation and acid-base balance," *Br. J. Anaesth.* **74**(5), 591–606 (1995).
2. T. Gys, A. Hubens, H. Neels, L. F. Lauwers, and R. Peeters, "Prognostic value of gastric intramural pH in surgical intensive care patients," *Crit. Care Med.* **16**(12), 1222–1224 (1988).
3. G. R. Doglio, J. F. Pusajo, M. A. Eguurrola, G. C. Bonfigli, C. Parra, L. Vetere, M. S. Hernandez, S. Fernandez, F. Palizas, and G. Gutierrez, "Gastric mucosal pH as a prognostic index of mortality in critically ill patients," *Crit. Care Med.* **19**(8), 1037–1040 (1991).
4. G. Gutierrez, F. Palizas, G. Doglio, J. Pusajo, N. Wainsztein, F. Klein, A. Galesio, J. Pacin, B. Dorfman, A. Dubin, E. Schiavi, J. Shottender, M. Jorge, J. Pusajo, "Gastric intramucosal pH as a therapeutic index of tissue oxygenation in critically ill patients," *Lancet* **339**(8787), 195–199 (1992).
5. J. C. Puyana, B. R. Soller, B. Parikh, and S. O. Heard, "Directly measured tissue pH is an earlier indicator of splanchnic acidosis than tonometric parameters during hemorrhagic shock in swine," *Crit. Care Med.* **28**(7), 2557–2562 (2000).
6. X. Marechal, S. Mordon, J. M. Devoisselle, S. Begu, B. Guery, R. Nevriere, B. Buys, G. Dhelin, J. C. Lesage, D. Mathieu, and C. Chopin, "In vivo application of intestinal pH measurement using 2',7'-bis(carboxyethyl)-5,6-carboxyfluorescein (BCECF) fluorescence imaging," *Photochem. Photobiol.* **70**(5), 813–819 (1999).
7. M. R. James-Kracke, "Quick and accurate method to convert BCECF fluorescence to pH: calibration in three different types of cell preparations," *J. Cell Physiol.* **151**(3), 596–603 (1992).
8. R. Y. Tsien, "Fluorescent indicators of ion concentrations," *Methods Cell Biol.* **30**, 127–156 (1989).
9. J. A. Bonanno and K. A. Polse, "Measurement of in vivo human corneal stromal pH: open and closed eyes," *Invest. Ophthalmol. Visual Sci.* **28**(3), 522–530 (1987).
10. D. A. Russell, R. H. Pottier, and D. P. Valenzeno, "Continuous non-invasive measurement of in vivo pH in conscious mice," *Photochem. Photobiol.* **59**(3), 309–313 (1994).
11. R. B. Silver, "Ratio imaging: practical considerations for measuring intracellular calcium and pH in living tissue," *Methods Cell Biol.* **56**, 237–251 (1998).
12. G. R. Bright, G. W. Fisher, J. Rogowska, and D. L. Taylor, "Fluorescence ratio imaging microscopy," *Methods Cell Biol.* **30**, 157–192 (1989).
13. G. R. Martin and R. K. Jain, "Fluorescence ratio imaging measurement of pH gradients: calibration and application in normal and tumor tissues," *Microvasc. Res.* **46**(2), 216–230 (1993).
14. A. Bogaards, M. C. Aalders, C. C. Zeyl, S. de Blok, C. Dannecker, P. Hillemanns, H. Stepp, and H. J. Sterenborg, "Localization and staging of cervical intraepithelial neoplasia using double ratio fluorescence imaging," *J. Biomed. Opt.* **7**(2), 215–220 (2002).
15. S. Bégu-Soulie, "Caractérisation physico-chimique de marqueurs fluorescents pH-sensibles: application à l'étude de la capture hépatique des liposomes," in *Biologie Santé*, p. 214, Université de Montpellier, Montpellier (1997).
16. X. Maréchal, "Mise en oeuvre d'une technique de cartographie du pH tissulaire par imagerie de fluorescence," in *L'université technologique de Compiègne*, p. 813, Université technologique de Compiègne, Compiègne (2000).
17. Y. L. Lai, E. D. Martin, B. A. Attebery, and E. B. Brown, Jr., "Mechanisms of extracellular pH adjustments in hypercapnia," *Respir. Physiol.* **19**(2), 107–114 (1973).
18. W. B. Schwartz, "Defense of extracellular pH during acute and chronic hypercapnia," *Ann. N.Y. Acad. Sci.* **133**(1), 125–133 (1966).
19. J. B. Anyonsson, C. C. Boyle III, K. L. Kuki, S. Endo, K. Yoshida, K. Yamamoto, and H. Matsuda, "Validation of tonometric measurement of gut intramural pH during endotoxemia and mesenteric occlusion in pigs," *Am. J. Physiol.* **259**, 519–523 (1990).
20. J. A. Guzman and J. A. Kruse, "Gut mucosal-arterial Pco₂ gradient as an indicator of splanchnic perfusion during systemic hypo- and hypercapnia," *Crit. Care Med.* **27**(12), 2760–2765 (1999).
21. T. Kishimoto, Y. Fujino, S. Nishimura, N. Taenaka, and T. Mashimo, "Validity of gastric intramucosal pH (pHi) for circulatory evaluation in pediatric patients," *J. Clin. Monit. Comput.* **17**(2), 87–92 (2002).
22. T. Masai, K. Taniguchi, S. Kuki, S. Endo, K. Yoshida, K. Yamamoto, and H. Matsuda, "Gastric intramucosal pH during lower body circulatory arrest under open distal anastomosis with selective cerebral perfusion in aortic arch repair," *ASAIO J.* **47**(5), 548–551 (2001).